Infrared emission of hot water in the atmosphere of Mira

Yamamura, I.; de Jong, T.; Cami, J.

Published in:
Astronomy & Astrophysics

The Astrophysical Journal, 579:446–454, 2002 November 1

EVIDENCE FOR VERY EXTENDED GASEOUS LAYERS AROUND O-RICH MIRA VARIABLES AND M GIANTS

B. Mennesson,[1] G. Perrin,[2] G. Chagnon,[2] V. Coude du Foresto,[2] S. Ridgway,[3] A. Merand,[2] P. Salome,[2] P. Borde,[2] W. Cotton,[4] S. Morel,[5] P. Kervella,[5] W. Traub,[6] and M. Lacasse[6]

Received 2002 March 15; accepted 2002 July 3

ABSTRACT

Nine bright O-rich Mira stars and five semiregular variable cool M giants have been observed with the Infrared and Optical Telescope Array (IOTA) interferometer in both K' ($\sim$2.15 μm) and L' ($\sim$3.8 μm) broadband filters, in most cases at very close variability phases. All of the sample Mira stars and four of the semiregular M giants show strong increases, from $\simeq$20% to $\simeq$100%, in measured uniform-disk (UD) diameters between the K' and L' bands. (A selection of hotter M stars does not show such a large increase.) There is no evidence that K' and L' broadband visibility measurements should be dominated by strong molecular bands, and cool expanding dust shells already detected around some of these objects are also found to be poor candidates for producing these large apparent diameter increases. Therefore, we propose that this must be a continuum or pseudocontinuum opacity effect. Such an apparent enlargement can be reproduced using a simple two-component model consisting of a warm (1500–2000 K), extended (up to $\simeq$3 stellar radii), optically thin ($\tau \simeq 0.5$) layer located above the classical photosphere. The Planck weighting of the continuum emission from the two layers will suffice to make the L' UD diameter appear larger than the K' UD diameter. This two-layer scenario could also explain the observed variation of Mira UD diameters versus infrared wavelength—outside of strong absorption bands—as already measured inside the H, K, L, and N atmospheric windows. This interpretation is consistent with the extended molecular gas layers (H_2O, CO, etc.) inferred around some of these objects from previous IOTA K'-band interferometric observations obtained with the Fiber Linked Unit for Optical Recombination (FLUOR) and from *Infrared Space Observatory* and high-resolution ground-based FTS infrared spectra. The two-component model has immediate implications. For example, the Mira photosphere diameters are smaller than previously recognized—this certainly implies higher effective temperatures, and it may favor fundamental mode pulsation. Also, the UD model fails generally to represent the brightness distribution and has very limited applicability for Mira stars. The presence of a very extended gas layer extending up to $\simeq$3 stellar radii seems now well established on a fair sample of asymptotic giant branch stars ranging from late-type giants to long-period variables, with some probable impact on stellar model atmospheres and mass-loss mechanisms.

Subject headings: circumstellar matter — instrumentation: interferometers — stars: atmospheres — stars: variables: other — techniques: interferometric

1. INTRODUCTION

Because of their large angular scale and unusually high infrared brightness, late-type stars, and particularly Mira variables, have been extensively observed in the near-infrared to thermal infrared using high angular resolution imaging techniques. Many such observations have been reported lately, using either single-telescope aperture masking (Tuthill, Haniff, & Baldwin 1995, 1999a; Tuthill et al. 2000a; Haniff, Scholz, & Tuthill 1995), direct near-infrared long-baseline interferometry (e.g., Perrin et al. 1999; Young et al. 2000), or mid-infrared heterodyne interferometry (Danchi et al. 1994; Lopez et al. 1997; Weiner et al. 2000). From this body of work emerges a very complex description of the stellar photosphere and near-in environments of Mira variables, with repeated occurrences of strong asymmetries, large chromatic size variations (particularly pronounced in regions of deep molecular absorption by species such as TiO or VO), evidence for clumps, hot spots, and of course phase variability of the whole structure. Consequently, the modeling of generally partial (in azimuth or spatial frequency) visibility measurements is very delicate, and many fundamental aspects of Mira variables still remain unclear. This is illustrated by the continuing debate on the pulsation mode of these objects (Willson 2000; Whitelock & Feast 2000; Wood 1999) and the difficulties of fitting the data with existing limb-darkening models. As already stated (Hofmann, Scholz, & Wood 1998), one major problem arises from the difficulty of retrieving accurate Rosseland diameters and corresponding physical characteristics—such as effective temperatures or modes of pulsation—from interferometric observations at monochromatic

[1] Jet Propulsion Laboratory, California Institute of Technology, MS 306-388, 4800 Oak Grove Drive, Pasadena, CA 91109; bertrand.mennesson@jpl.nasa.gov.

[2] Laboratoire d'Etudes Spatiales et d'Instrumentation en Astrophysique, 5 Place Jules Janssen, F-92195 Meudon, France; guy.perrin@obspm.fr, gilles.chagnon@obspm.fr, vincent.foresto@obspm.fr, merand@clipper.ens.fr, philippe.salome@obspm.fr, pascal.borde@obspm.fr.

[3] National Optical Astronomy Observatory, Tucson, AZ 85719; ridgway@noao.edu.

[4] National Radio Astronomy Observatory, 520 Edgemont Road, Charlottesville, VA 22903-2475; bcotton@nrao.edu.

[5] European Southern Observatory, Karl-Schwartzschild Strasse 2, 85748 Garching, Germany; pkervell@eso.org, smorel@eso.org.

[6] Harvard-Smithsonian Center for Astrophysics, Cambridge, MA 02138; traub@cfa.harvard.edu, lacasse@cfa.harvard.edu.

wavelengths or in various broadband filters. The effects of limb darkening, atmospheric extension, and variability phase are very difficult to implement in the models, especially close to strong molecular absorption lines (see for instance the effect of TiO at 710 nm in Haniff et al. 1995). One hope was that infrared measurements would be less sensitive to limb-darkening effects and whould provide less contaminated or true "photosphere" size estimates, commensurate with Rosseland diameters and rather constant versus wavelength or phase (Tej et al. 1999). Unfortunately, angular diameters measured in the infrared show complex behaviors similar to optical diameters, as already suggested by previous measurements of individual stars (Tuthill et al. 1999b, 2000b; Mennesson et al. 1999b) and extensively reported in this paper. Yet we believe that the chromatic dependence of Mira star apparent uniform-disk diameters in the near-infrared, especially in the 2–4 μm region, can be efficiently used to constrain the near-in stellar atmospheric structure. This is illustrated by the following analysis of our K'/L' band data, related to other high angular or spectral resolution measurements when available.

In the next section we briefly describe our observational setup. We present the experimental results in § 3 and give a general interpretation of these in § 4, in comparison with relevant models and observations.

2. OBSERVATIONS

All measurements presented here were acquired on the Infrared and Optical Telescope Array (IOTA: Traub 1998) with baselines ranging from 15 to 38 m. They used the FLUOR single-mode guided optics instrument (Perrin 1996; Coudé du Foresto et al. 1998) in the K' or K band (2.0–2.4 μm) and the "Thermal Infrared Stellar Interferometric Setup" (TISIS), FLUOR's extension to the L' band (3.4–4.1 μm). The L'-band experiment saw first light in 1998 April (Mennesson et al. 1999a). All L' data reported here were obtained in 2000 with an upgraded version using a dedicated L' single-mode coupler and slow background chopping (0.01–0.1 Hz, which was found to be sufficient for bright objects) with IOTA tertiary mirrors. 2000 November data used the two complementary interferometric outputs and are of better quality than those obtained in 2000 March with a single photometer. FLUOR monitors both the incoming flux coming from each telescope and the interferometric fluxes. In contrast to FLUOR, TISIS uses a simple single-mode fluoride glass coupler and measures only the interferometric signals. Owing to this lack of absolute photometric calibration, TISIS achieves a mean relative accuracy of 1%–5% on visibility measurements, to be compared to 1% or better with FLUOR.

Unless specified in the results, the characteristics of these K' and L' filters are the following: K' ($\lambda_{\rm mean} = 2.16$ μm, FWHM $= 0.32$ μm, and $\lambda_{\rm eff} = 2.13$ μm), L' ($\lambda_{\rm mean} = 3.79$ μm, FWHM $= 0.54$ μm, and $\lambda_{\rm eff} = 3.77$ μm). FLUOR measurements carried out before 2000 used a regular K filter ($\lambda_{\rm mean} = 2.20$ μm, FWHM $= 0.44$ μm, and $\lambda_{\rm eff} = 2.15$ μm). The effective wavelength $\lambda_{\rm eff}$ sets the observing spatial frequency at a given baseline. For a definition of $\lambda_{\rm eff}$ and of the general data reduction of broadband interferograms obtained with single-mode wave guides, please refer to Coudé du Foresto, Ridgway, & Mariotti (1997) and Perrin et al. (1998).

3. EXPERIMENTAL RESULTS

The azimuth coverage of the observations is small (below 30°) in all cases. In addition, we generally do not fully resolve the stars in L', with the sole exception of χ Cygni. Therefore, we chose to represent the data set by uniform-disk (UD) best fits. They should just be regarded as raw parameters for a preliminary diagnosis and analysis of the atmospheric structure. Using UD fits also avoids the modeling difficulty encountered when deriving Rosseland diameters from visibility measurements (Hofmann et al. 1998), mostly, in this case, where only first-lobe measurements are available, i.e., low-resolution information on the center-to-limb variation. Besides, chromatic variations in UD diameters are obviously related to true physical variations in stellar atmospheric structure with wavelength. Tables 1 and 2 show a summary of the results obtained in the two observing runs of 2000 February/March and 2000 October/November. Note that in some cases—R Cassiopeiae, χ Cygni, o Ceti, R Leonis, and RS Cancri in 2000 November—the quoted error bars on the UD diameters are asymmetric and much larger than the formal error bars deduced from a least-squares fit of the visibility data. That is because these stars were found to depart strongly from UD models, and we preferred to give L'-band UD diameter *intervals* in that case. The mean UD diameter is computed using all spatial frequencies available. The UD diameter "error bar" is given by the smallest and largest UD diameters obtained when fitting each visibility point individually. For the other stars in the sample, either a single spatial frequency was observed (R Aquarii, U Herculis, R Cancri, R Leonis Minoris, RT Virginis, RX Bootis, g Herculis, and RS Cancri in 2000 March) or no significant departure from UD models was detected (U Orionis and SW Vir), which seems to be the exception. In these two cases, the quoted error bar on the UD diameter comes directly from the least-squares fit residuals, using all visibility points available. Luminosity phases were determined using the AFOEV[7] database. For each observing campaign, all stars have been observed in the two spectral channels within 25 days maximum, with the exception of R Leonis and RS Cancri. Additional measurements obtained at other phases or in different filters with FLUOR/TISIS are also given for R Leonis and o Ceti.

3.1. *General Results*

An exhaustive list of L' visibility measurements obtained with TISIS on Mira variables, supergiants, and semiregular variable red giants will be given in a forthcoming paper (Chagnon et al. 2001). We concentrate here on the observational results obtained on evolved stars. Yet, owing to the importance of the chromatic size variations reported here, it is worthwhile noting that no similar variations with phase or wavelength have been detected by the FLUOR and TISIS instruments on any giants or supergiants with a type earlier than M5. This is illustrated, for instance, by K'/L' measurements of the M5 II supergiant α Herculis, showing no variation in UD diameters at the 1% level (G. Perrin et al., in preparation). We also note that in contrast to Mira variables, these earlier type stars show L'-band visibility curves in very good agreement with UD models.

[7] AFOEV: Association Francaise des Observateurs d'Etoiles Variables.

TABLE 1
UD Diameter Best Fits (ϕ) Obtained for Nine Mira Variables Using K' and L' FLUOR/TISIS Measurements

Star	Spectral Type	Date	Variable Phase	Filter	ϕ (mas)
R Aquarii	M7 IIIpevar (Mira)	2000 Oct 18	0.41	K'	16.88 ± 0.56
		2000 Nov 20	0.51	L'	34.32 ± 1.09
R Cassiopeiae	M7 IIIe (Mira)	2000 Oct 14–15	0.09	K'	24.78 ± 0.09
		2000 Nov 14–23	0.17	L'	$31.09^{+2.58}_{-4.31}$
U Herculis	M7 III (Mira)	2000 Feb 19–26	0.23	K'	10.98 ± 0.01
		2000 Mar 10	0.27	L'	14.26 ± 0.47
χ Cygni	S (Mira)	2000 May 15–24	0.38	K'	23.24 ± 0.08
		2000 Nov 14–23	0.81	L'	$30.40^{+3.30}_{-7.28}$
R Cancri	M7 IIIe (Mira)	2000 Feb 26	0.34	K'	11.58 ± 0.02
		2000 Mar 11	0.37	L'	16.59 ± 0.42
		2000 Oct 16	0.96	K'	10.04 ± 0.08
		2000 Nov 20	1.06	L'	13.39 ± 2.45
R Leonis Minoris	M7e (Mira)	2000 Feb 19	0.37	K'	11.85 ± 0.01
		2000 Oct 16	0.97	K'	10.48 ± 0.05
		2000 Nov 20	1.08	L'	21.44 ± 0.70
U Orionis	M8 III (Mira)	2000 Oct 15–18	0.88	K'	15.59 ± 0.06
		2000 Nov 15–20	0.96	L'	25.66 ± 0.69
o Ceti	M7 IIIe (Mira)	1997 Dec 19	0.94	K	28.79 ± 0.10
		2000 Oct 18	4.02	2.03 μm	25.73 ± 0.09
		2000 Oct 18	4.02	2.15 μm	25.13 ± 0.08
		2000 Oct 18	4.02	2.22 μm	25.19 ± 0.12
		2000 Oct 18	4.02	2.39 μm	29.22 ± 0.12
		2000 Oct 18	4.02	K'	24.40 ± 0.11
		2000 Nov 14–23	4.11	L'	$35.21^{+2.75}_{-1.27}$
R Leonis	M8 IIIe (Mira)	1996 Apr 17–18	0.24	K	28.18 ± 0.05
		1997 Mar 4	1.28	K	30.68 ± 0.05
		2000 Mar 10–14	4.81	L'	$36.02^{+0.43}_{-0.52}$
		2000 Nov 14–22	5.62	L'	$39.08^{+1.49}_{-3.30}$

Note.—Variability phases are averaged over the time of the observations. For o Ceti narrowband measurements around 2.03, 2.15, 2.22, and 2.39 μm, the filters FWHM is $\simeq$100 nm.

3.1.1. *UD Diameter versus Wavelength*

All of the O-rich Mira stars in the sample (eight of spectral type M and one, χ Cygni, of spectral type S) and four of the M giant semiregular variables (SW Virginis, RT Virginis, RX Bootis, and g Herculis) show the same trend (Tables 1 and 2): a large (>20%) increase in UD diameter between K' and L'. The amplitude of the effect varies strongly with the star. R Aquarii and R Leonis Minoris clearly stand out in the sample with enlargements from K' to L' of $\simeq$100% at variability phases differing by only 0.10. The detailed circumstellar structure obviously differs from one star to another, with peculiar characteristics in some cases—e.g., R Aquarii is a symbiotic star—but there could be a common simple cause for such a systematic effect.

Note that for R Leonis and RS Cancri, the K' and L' observations were not conducted at close variability phases. Each of the R Leonis K' measurements provides size esti-

TABLE 2
UD Diameters Best Fits (ϕ) Obtained for Five Semiregular Variables (b Type)[a] Using K' and L' FLUOR/TISIS Measurements

Star	Spectral Type	Date	Filter	ϕ (mas)
SW Virginis	M7 III (SR b)	2000 Feb 29	K'	16.24 ± 0.06
		2000 Mar 9–14	L'	22.88 ± 0.33
RT Virginis	M8 III (SR b)	2000 Feb 18	K'	12.38 ± 0.13
		2000 Mar 11	L'	16.24 ± 0.73
RX Bootis	M7.5 III (SR b)	2000 Feb 29	K'	17.48 ± 0.13
		2000 Mar 10–12	L'	21.00 ± 0.27
g Herculis	M6III (SR b)	2000 Feb 27	K'	12.67 ± 0.04
		2000 Mar 12	L'	20.84 ± 0.59
RS Cancri	M6 IIIase (SR b)	1996 Apr 17	K'	14.27 ± 0.09
		2000 Mar 14	L'	21.71 ± 1.09
		2000 Nov 17–22	L'	$14.81^{+3.22}_{-2.93}$

[a] By definition one cannot give accurate luminosity phases for these objects.

mates noticeably smaller than in L' though, implying that this effect is real. For RS Cancri, more observations will be required to reach a conclusion about the K'/L' behavior.

3.1.2. *UD Diameters versus Variability Phase*

Four Mira stars have been observed at different variability phases in K' and/or L': R Cancri, R LMi, o Ceti, and R Leonis. In all cases the apparent UD diameter is larger when the star is observed closer to its luminosity minimum. This effect is also observed in L' on the only semiregular variable that was observed at two different epochs, RS Cancri. Although these first results may indicate a trend, the time coverage is not yet sufficient to draw conclusions.

3.1.3. *Study of Possible Correlations*

The L'-to-K' UD diameter ratio was investigated for possible correlation with a number of parameters, namely, the star variability phase, variability period, infrared excess, spectral type, visible magnitude variation amplitude (as provided by the records of the AFOEV), and mass-loss rate. We used the stellar physical parameters listed in Table 3. Magnitude differences between 12 and 25 μm were derived from *IRAS* measurements (Beichman et al. 1988) using the same relation as in Walker & Cohen (1988), i.e., $[12] - [25] = 1.56\text{–}2.5 \log(F_{12}/F_{25})$, with F_{12} and F_{25} the *IRAS* fluxes in Janskys at 12 and 25 μm. Phases given are mean visible luminosity phases at the time of K' or L' observations. For R Leonis and RS Cancri no K'/L' observations at close phases are available, and diameter error bars reflect measurements at different epochs of the cycle. Mass-loss rates estimates are taken from Loup, Forveille Omont, & Paul (1993) or from Le Bertre & Winters (1998).

The conclusion is that no strong correlation was found between the UD diameter ratio and any of these parameters. A possible exception is the mass-loss rate, for which a weak correlation was found. Note, however, that for different authors and methods of computation (radio observations of CO emission lines, empirical photometric relations, etc.), there is a large scatter of mass-loss rate estimates in the literature (generally within a factor of 3 or more), so the correlation with this parameter is difficult to assess.

3.2. *Individual Stars Results*

As representative examples of the effects reported here, we present the visibility curves and UD diameter estimates obtained in K' and L' for o Ceti, R Aquarii, and R Leonis, three very well-known Mira stars that have been observed extensively at high resolution from the near-infrared to the radio domain.

3.2.1. *o Ceti*

Figure 1 shows visibilities measurements and best UD fits in K' (2000 October) and L' (2000 November) bands for o Ceti; o Ceti is a Mira prototype star with a spectral type M7 IIIe and a period of 332 days. We observed it close to its maximum variability phase in 2000 October/November, yielding UD diameter fits of 24.40 ± 0.11 mas in K' and $35.21^{+2.75}_{-1.27}$ mas in L'. The observed enlargement with increasing wavelength is then 44% for variability phases differing by only 0.09. The K-band UD diameter previously measured in 1997 December is also consistent with a much smaller apparent size in K band, although no L' measurements were available at the same epoch. Data obtained in 1998 December with an earlier less accurate version of TISIS also confirm the larger L' diameter (Mennesson et al. 1999b), so the the chromatic effect is now well established. The *Infrared Space Observatory* (*ISO*) spectrum (Yamamura, de Jong, & Cami 1999) of o Ceti does not show any significant absorption features in the region covered by the L' filter: only the very edges are contaminated by residual

TABLE 3

PHYSICAL PROPERTIES OF MIRA VARIABLES AND SEMIREGULAR VARIABLE STARS OBSERVED WITH FLUOR/TISIS

Star	Period (days)	$[12] - [25]$	dM/dt ($M_\odot$ yr^{-1})	Δm_V	Phase	$\phi_{L'}/\phi_{K'}$
R Aquarii	387	0.40	$3.0\,10^{-7}$[a]	5	0.46 ± 0.05	$2.03^{+0.14}_{-0.12}$
R Cassiopeiae	431	0.60	$1.1\,10^{-6}$[b]	7	0.13 ± 0.04	1.25 ± 0.01
U Herculis	405	0.45	$2.6\,10^{-7}$[b]	6.5	0.25 ± 0.02	1.30 ± 0.05
χ Cygni	408	0.15	$5.6\,10^{-7}$[b]	8.5	0.59 ± 0.22	1.31 ± 0.01
R Cancri	362	0.49	$2.0\,10^{-8}$[a]	5	0.36 ± 0.02	1.43 ± 0.04
					0.01 ± 0.05	1.33 ± 0.12
R Leonis Minoris	372	0.60	$2.8\,10^{-7}$[b]	5.5	0.03 ± 0.05	2.04 ± 0.05
U Orionis	372	0.51	$3.0\,10^{-7}$[a]	6.5	0.92 ± 0.04	1.65 ± 0.02
o Ceti	332	0.72	$5.0\,10^{-7}$[a]	7	0.06 ± 0.05	1.44 ± 0.01
R Leonis	310	0.26	$1.0\,10^{-7}$[b]	5.5	...	1.28 ± 0.11
SW Virginis	150	0.81	$5.7\,10^{-7}$[b]	2.5	...	1.41 ± 0.02
RT Virginis	...	0.77	$7.4\,10^{-7}$[b]	1	...	1.31 ± 0.06
RX Bootis	195	0.80	$8.1\,10^{-7}$[b]	1.5	...	1.20 ± 0.01
g Herculis	89	0.39	$2.6\,10^{-7}$[b]	1	...	1.64 ± 0.05
RS Cancri	120	0.66	$5.2\,10^{-7}$[b]	1.5	...	$1.28^{+0.33}_{-0.27}$
Correlation factor	0.145	−0.133	−0.344	0.084	0.114	

NOTE.—The last line indicates the correlation coefficient between the measured L' to K' UD diameter ratios ($\phi_{L'}/\phi_{K'}$) at a given luminosity phase, and the various stellar parameters. For R Leonis and RS Cancri measurements are not obtained at close phases, so all observations are used to derived UD diameter ratios. $[12] - [25]$ mag differences are derived from *IRAS* measurements (see text); Δm_V is the typical stellar visible magnitude variation during one luminosity cycle.

[a] Stellar mass-loss rates estimate from Le Bertre & Winters 1998.

[b] Stellar mass-loss rates estimate from Loup et al. 1993.

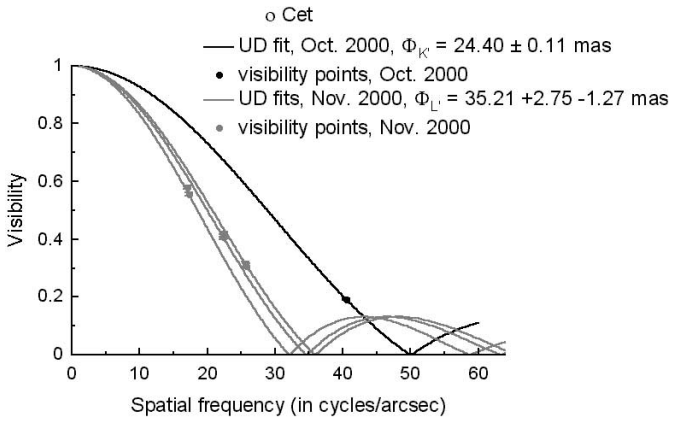

FIG. 1.—o Ceti observations: 2000 October (K') and November (L'). Visibility measurements and best UD fits. A significant departure from the UD model is visible in the L' data. The mean UD L' diameter is computed using the three available spatial frequencies. The L' UD diameter error bar is given by the smallest and largest UD diameters obtained when fitting each visibility point individually.

OH and SiO absorptions. Similarly, our FLUOR narrowband data (Table 1; G. Perrin et al., in preparation) show a small difference between K' broadband UD diameter and narrowband UD diameters measured in the "continuum" around 2.15 and 2.22 μm. This shows that o Ceti broadband K' diameter estimates are fairly unaffected by substantial molecular absorption. The strong effect of CO and H_2O appears only in the 2.39 μm narrowband measurements, at the very edge of the K' filter.

3.2.2. *R Aquarii*

Figure 2 shows visibility measurements and best UD fits in K (2000 October) and L' (2000 November) bands for R Aquarii, a mass-losing long-period ($\simeq$387 days) Mira variable, with a spectral type M7 III. R Aquarii is believed to be in a symbiotic system. Recent aperture-masking measurements (Tuthill et al. 2000a) placed an upper limit of around $\Delta_M > 5$ mag for the relative infrared (J to K) brightness of the potential companion. We observed R Aquarii close to its minimum variability phase in 2000 October/November, yielding UD diameter fits of 16.88 ± 0.56 mas in K and 34.32 ± 1.09 mas in L', which represents a relative enlargement of 103% for variability phases differing by only 0.10.

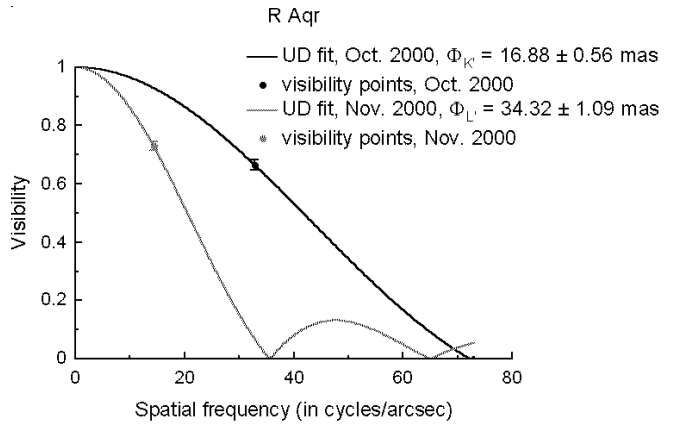

FIG. 2.—R Aquarii observations: 2000 October (K') and November (L'): visibility measurements and best UD fits.

This enlargement may be due to the continuum emission of an upper layer contributing a significant fraction of the stellar flux as wavelength increases—our favored model discussed at greater length below—or may indicate the presence of a cold companion, visible only at longer infrared wavelength. This last assumption is consistent with the significant deviation from circular symmetry found by aperture masking at 3.08 μm and not at shorter wavelengths.

3.2.3. *R Leonis*

R Leonis is a Mira star of spectral type M8 IIIe with a period of 310 days. This is the only case in our sample where UD diameter measurements in K' and L' were taken at substantially different phases. Yet they show the same trend as the other stars: a marked increase in size from K to L', of the order of 20%–30%. K-band data recorded in 1996 April and 1997 March were analyzed previously (Perrin et al. 1999). These data showed size variability with phase and residual visibilities at high spatial frequency. They were best fitted using an extended brightness distribution, as derived in models of molecular scattering by CO and H_2O (Hofmann et al. 1998). We also note that the apparent UD diameter in L' increases by 9% between phases 0.81 and 1.62 during the 2000 observations. These fluctuations with phase may be due to changes in the spatial extent—and/or in opacity—of the outer atmospheric layers, as already deduced for R Leonis and χ Cygni from Cambridge Optical Aperature Synthesis Telescope (COAST) interferometric observations (Burns et al. 1998; Young et al. 2000) at 830 and 910 nm. K' visibility variations may trace actual variations in the size of the deeper continuum forming layers, while L' variations may reflect opacity or temperature variations in an extended envelope. Accurate modeling of the center-to-limb variation at each wavelength and improved spatial frequency coverage in the interferometric measurements are necessary to disentangle these two effects.

The 1997 March and 2000 November data, which provide the best spatial frequency coverage in each of the K' and L' bands, are presented and modeled in more detail in § 4.1.3.

3.2.4. *RS Cancri*

Uniquely among our observations of semiregular variables, RS Cancri shows a large change in the L' visibility and implied UD diameter, and this is for observations at similar "phase" separated by two full cycles. Although the variation is much larger than the estimated errors, such a large variation does seem surprising, and this result should be confirmed before drawing conclusions.

4. DISCUSSION

4.1. *Interpretation*

We are seeking here to advance one general explanation for the observed diameter changes between the K' and L' bands.

4.1.1. *General*

Substantial absorption lines of molecular H_2O, CO, SiO, and CO_2 are visible in some O-rich Mira variable near-infrared spectra (Yamamura et al. 1999; Tsuji et al. 1997), but they appear outside the K' and L' filters. Even though some wing absorption features may still be present, the overall stellar flux remains largely overwhelmed by continuum

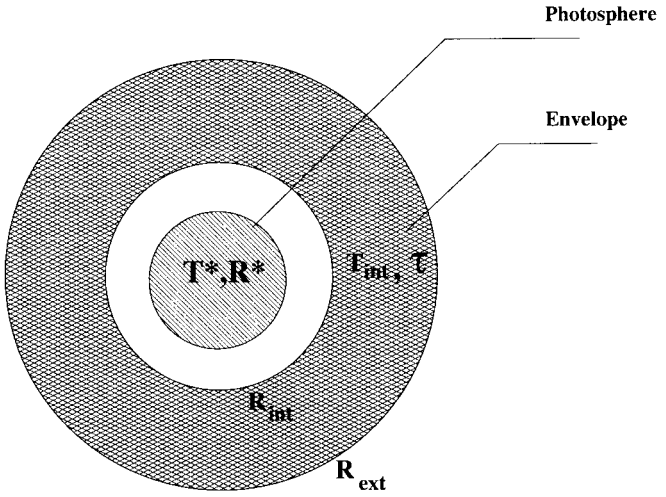

FIG. 3.—Adopted spherically symmetric model. It consists of a central photosphere with radius R^* and effective temperature T^*, surrounded by an envelope with inner radius $R_{\rm int}$, outer radius $R_{\rm ext}$, inner temperature $T_{\rm int}$, and optical depth τ, common to both K' and L' bands.

emission for broadband observations in any of the H, K', and L' filters (Scholz 2001).

There is no evidence for molecular bands strong enough to produce large opacity difference between the K' and L' broadband regions, so the broadband diameters measured in these filters should be very close to continuum size measurements.

In the absence of obvious strong molecular absorption, the effective opacity in the broad-filter bandpasses may be determined by the continuum, or possibly by a large number of weak, overlapping, and blended lines that form a pseudo-continuum. This leads us to an interpretation based on a continuum effect. We propose a model consisting of a cool, semitransparent gaseous shell extending far above the classical photosphere, typically 3 stellar radii away (Fig. 3). We suggest that the Planck weighting of the emission from the two layers will suffice to make the L' UD diameter appear larger than the K' UD diameter. Owing to the wavelength dependence of the Planck function, the extended cooler ($\simeq$1500–2000 K) gas layer contributes a larger fraction to the overall stellar flux at 3.8 μm than at 2.2 μm for instance. More generally, when the star is observed in infrared regions that are beyond the peak emission of the "classical" photosphere ($\lambda > 1$–1.5 μm), emission from this extended region can become important. The variation in apparent size with wavelength is then a temperature effect modulating the relative contribution from the extended atmosphere. Aside from a general increase in apparent size with wavelength, the detailed variation with wavelength should be diagnostic of the opacity source. Thus a molecular pseudo-continuum would be effective only in wavelength regions where line opacity was important.

4.1.2. *The Example of R Leonis*

Interestingly, the circumstellar gas layer does not need to be optically thick to produce a substantial apparent diameter increase between the K' and L' atmospheric windows. This is illustrated by simple models for R Leonis. The physical model consists of the central photosphere considered as a blackbody with effective temperature T^* and radius R^* and a spherically symmetric surrounding envelope characterized by inner radius $R_{\rm int}$, outer radius $R_{\rm ext}$, inner temperature $T_{\rm int}$, and optical depth τ common to both K' and L' bands (Fig. 3). That is six free parameters, to be compared with the 11 true independent R Leonis visibility measurements we have. To keep the model simple, we assumed radiative equilibrium and mass flux conservation inside an assumed expanding envelope, so the the temperature there varies as $1/\sqrt{r}$ and the density goes as $1/r^2$. The numerical code solves for the one-dimensional radiative transfer equation for each line of sight separately and sums the resulting intensities to provide the center-to-limb variation (CLV).

As an example, Figure 4 shows the CLV and visibility curves obtained when fitting the K' (1997 March) and L' (2000 November) R Leonis data with such a model. A reasonably good fit (χ^2 per point of 2.2) is found with a 10 mas radius uniform photosphere at an effective temperature of 2700 K, surrounded by a spherical layer extending from 15 to 27 mas, with an inner temperature of 1730 K and an optical depth of $\simeq$0.5 in both K' and L'. Figure 4*a* shows the increased relative contribution of the upper layer flux at 3.8 μm. Looking at the visibility curves (Fig. 4*b*), the outer layer affects the mid-spatial frequencies but has no influence on

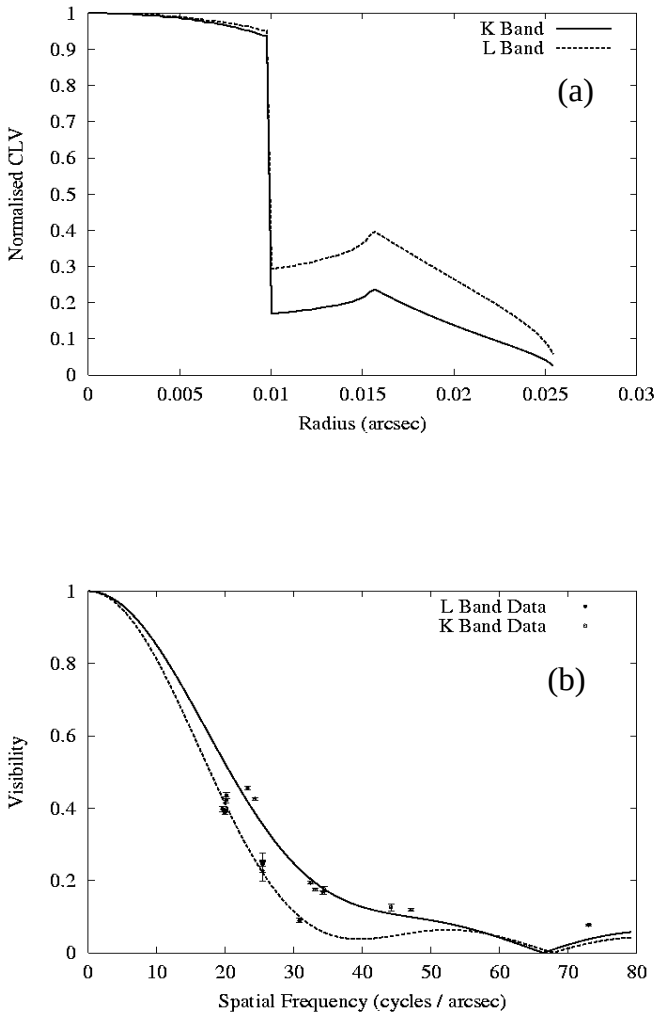

FIG. 4.—Results of R Leonis observations modeling using a two-layer model (see text). Predicted CLV and visibility curves are given by the solid line in K and by the dashed line in L'. (*a*) Center-to-limb variation. (*b*) Model visibility and observations: 1997 March (K') and 2000 November (L').

the first visibility null location, which is fixed by the size of the photosphere. In that sense CLV curves appear as a good tool for disentangling the opacity variations in the outer atmosphere and the actual photospheric pulsation. We note that the large visibility residual observed in K' at the highest spatial frequency remains poorly fitted. More observations in the [50–70] cycles arcsec^{-1} spatial frequency range would obviously be very helpful for determining whether the visibility effectively bounces after a first minimum or monotonically decreases in a more Gaussian fashion. This is part of an ongoing work with FLUOR/TISIS.

In the fit, the upper layer was not assumed at thermal equilibrium with the central photosphere, so its inner temperature was left as a free parameter. This is consistent with recent models of molecular gas layers around Mira variables (Willson 2000) and better fits the data than in the case where thermal equilibrium is assumed. Good fits with similar χ^2 were obtained with different combinations of photospheric and inner layer radii. But the layer extension (up 2–3 stellar radii) and optical depth (0.4–1) seemed to be well constrained by the data. The actual source of opacity (dust or molecules) was not discussed, and no scattering was included, so this crude model obviously needs more work. Yet its merit is to easily reproduce the observed L' enlargements with few parameters.

4.1.3. *Issues Raised by the Two-Layer Model*

There are two main issues brought up by such a model: the physical interpretation of the "gap" region between the two layers and the impact of the model on the stellar spectral energy distribution (SED).

We did not force the inner radius of the surrounding layer to coincide with the stellar radius. The resulting apparent gap (Fig. 3), which is required to better fit the R Leonis visibility data, could arise from several sources but is most easily understood as a drop of opacity with depth. Either the continuum opacity or a pseudocontinuum opacity could vary with depth owing to changing abundances of molecules, ionization, or excitation. Although we do not have a specific hypothesis to explain a continuum drop, we note that the layers are observed to have molecular abundance and temperature differences. A layer of reduced gas density inside $R_{\rm int}$, while conceivable, may not be plausible hydrodynamically.

The extended, partially transparent shell of the two-component model may have both absorption and scattering opacity—both will result in an increased apparent UD diameter. The absorption opacity, however, likely to be dominant in K' or L', will lead to thermal reemission at a lower temperature. This will result in an increased flux at longer wavelengths, and the SED will deviate from a blackbody spectrum. However, the flux in the longer wavelength region available to be absorbed and reemitted is small. Mira variables differ strongly from blackbodies anyway, and the changes in the SED may not be dramatic. Simulation of the SED is beyond the scope of this paper, but it clearly sets an upper limit to the broadband opacities in the envelope.

It is already well known that supergiant stars have angular diameter variation within strong molecular bands (Quirrenbach et al. 1993) and even within single strong atomic lines (Schmidtke 1987). Higher spectral resolution diameter measurements in the L' band and more detailed modeling would be required to confirm whether such a wavelength-dependent opacity effect could give the large visibility changes that are observed averaged over the K' and L' bands. Our limited measurements and modeling suggest that isolated band and line opacity may not suffice. Therefore, in our modeling we have assumed a continuum opacity effect—of course, the physical phenomenon could arise as a result of an effective pseudocontinuum of many blended spectral lines. H_2O is a natural candidate for this opacity, as discussed in §§ 4.3.1 and 4.3.2.

Our model is simple, but it has the advantage of capturing and parameterizing the basic physical phenomena—two layers with a Planck weighting—with minimal additional complication. It is inspired by and maintains qualitative consistency with the latest detailed Mira studies. At the same time, it avoids complex and possibly incomplete physics that is necessarily included in state-of-the art modeling.

4.1.4. *The Issue of Azimuthal Asymmetry*

The FLUOR measurements at K' and L' show very clearly that a UD model does not represent the actual brightness distribution across Mira stars. The UD diameter can have only limited usefulness—here, we have used it as an index to parameterize visibility curves recorded at different wavelengths but otherwise nearly constant parameters. For example, the approximately north-south baselines of IOTA, with near-transit observations, give nearly constant position angle. At IOTA, multiple baselines are observed by moving telescopes—not by supersynthesis—and hence at nearly constant position angle. If supersynthesis were used to observe multiple baselines, as has been done elsewhere, the different position angles would correspond to different baseline lengths and different spatial frequencies. In that case, use of a UD model would appear to give evidence for an azimuthal variation in stellar diameter even for a symmetric disk. Azimuthal asymmetry is certainly not ruled out for Mira stars, but sparse UV coverage and UD model fitting cannot demonstrate asymmetry, which may be merely an artifact of adopting the UD model.

4.2. *Comparison to Existing Models*

The "two-layer Planck weighting effect" described above has been recently and independently proposed (Scholz 2001) to produce strong chromatic dependency in some Mira CLV and corresponding visibility models. One of these models (P74200) (Hofmann et al. 1998; Bedding et al. 2001) predicts strong (up to a factor of 2, depending on measured spatial frequency) apparent UD diameter increases between H, K, and L bands due to a "tail" in the CLV of Mira stars observed close to maximum variability phase. The effect of this "tail" is very important at mid-spatial frequencies of the first visibility lobe, where most of our observations are conducted. This tail would be mainly due to an extended H_2O layer extending far above the classical photosphere, which is consistent with our interpretation. The parameters for this model are the following: pulsation mode = fundamental, period = 332 days, stellar mass = 1 $M_\odot$, nonpulsating parent star radius $R_p = 241\ R_\odot$, "surface radius" $= 5R_p$, luminosity $L = 4960\ L_\odot$, stellar radius = $1.04R_p$, and effective temperature = 3060 K. One should note, however, that a strong cycle-to-cycle variation is predicted by these models and that the expected K'-L' discrepancy varies considerably from one luminosity maximum to

the following for instance. The visibility curves predicted by these models are so distinctive that a few measurements at well-chosen spatial frequencies could test them efficiently. This will be the aim of future observations. The essential element of this model is then consistent with our interpretation: the K to L (and H to K) apparent diameter enlargements are evidence for a "tail" in the CLV, due in this case to an extended atmospheric molecular layer.

Recent dynamical models of Mira atmospheres (Willson 2000) allow the formation of molecules (out of radiative equilibrium) and dust in a so-called refrigerating region as close as 2 stellar radii, also making the near-in molecular layer scenario plausible.

4.3. *Comparison to Other Observations*

Infrared spectra of some Mira stars and other M giants show extended molecular (mostly H_2O) regions whose size and temperatures are fully consistent with the extended layer invoked in our model. Thermal infrared measurements show that dust alone should not strongly affect near-infrared (J to L') diameters of late-type stars. Also, they show UD diameters around 11.15 μm, even larger than those measured at near-infrared wavelengths. This is also in agreement with our interpretation.

4.3.1. *ISO Spectra*

Warm molecular envelopes have been revealed by *ISO* infrared spectra of several Mira variables (o Ceti, S Virginis) and semiregular variables (SW Virginis, RT Virginis) of our sample. Of particular interest is the o Ceti *ISO* spectrum (Yamamura et al. 1999) taken between 2.4 and 5.3 μm close to its maximum phase. These authors found a remarkably accurate fit to the observed spectrum using two spherically symmetric molecular gas layers located above the classical photosphere and placed on top of each other. The first envelope contains hot H_2O (2000 K) and SiO (2000 K), whereas the outer colder one is composed of H_2O (1400 K) and CO_2 (800 K). Other molecular species, such as OH and CO, are also visible in the spectrum but were not included in the model since their parameters are less constrained. The hot optically thick H_2O molecular envelope extends out to two stellar radii. It is seen in emission in the 3.4–4 μm region (our L' filter), whereas the 2.6–3.3 μm radiation is absorbed by the outer cold (1400 K) H_2O layer, extending out to 2.3 stellar radii.

Like o Ceti, SW Virginis has been observed by *ISO* in the 2.4–5.3 μm region. Tsuji et al. 1997 found the spectrum compatible with absorption or emission due to H_2O, CO, SiO, and CO_2 extended envelopes. The 2.7 μm absorption feature would be due to an H_2O envelope extending to 2 stellar radii with an excitation temperature of 1250 K, whereas excess emission in the 3.95–4.55 μm region is mainly explained by extended 2000 K CO and 1250 K CO_2 envelopes.

4.3.2. *Ground-based FTS Spectra*

Further independent evidence for extended gas layers around late-type stars comes from excess absorption in first overtone CO bands. It was measured by high-resolution FTS spectra of a few late M giants, including RX Bootis, SW Virginis, g Herculis, and ρ Persei (Tsuji 1988), and interpreted as the effect of a quasi-static molecular formation zone, an extra molecular component distinct from the photosphere and characterized by excitation temperatures in the 1000–2000 K range.

There is also strong indication of an analogous two-layer H_2O extended structure around R Leonis. This comes from high-resolution spectroscopy of the 1.9 μm H_2O band (Hinkles & Barnes 1979). These authors derived excitation temperatures of 1700 and 1150 K for the two components, i.e., somewhat similar to the hot and cold layers inferred around o Ceti (Yamamura et al. 1999).

4.3.3. *Aperture-Masking Observations*

Near-infrared narrowband (generally 1%–3% wide) aperture-masking observations on the Keck telescope were recently reported for o Ceti (Tuthill et al. 1999b) and R Aquarii (Tuthill et al. 2000a), two of our targets, as well as for W Hydrae (Tuthill et al. 2000b), another Mira.

When observed in the continuum, these three stars show a substantial ($\simeq$10%–20%) increase in apparent diameter between H and K. This is much more than what conventional differential limb darkening between H and K may account for, and it is consistent with what would be expected from a two-layer model.

In all cases again, measurements conducted around 3.08 μm show much larger objects than in K: the 3.08 μm UD best-fit diameter is 59.9 mas for o Ceti observed close to maximum phase in 1997 December and around 34 mas for R Aquarii observed at two different epochs (1998 June and 1999 January). This may be interpreted by substantial molecular absorption in the upper atmosphere (possibly by water vapor, in the wings of the 2.7 μm feature visible in o Ceti *ISO* spectra).

The aperture-masking observations also appear consistent with the presence of a very extended molecular gas layer around these stars.

4.3.4. *Thermal Infrared Interferometry*

Early 11.15 μm observations with the Infrared Spatial Interferometer (ISI) 13 m baseline were carried out on a sample of 13 late-type stars (Danchi et al. 1994). As expected from infrared excesses previously detected around Mira variables by *IRAS* (Little-Marenin & Little 1990), the ISI measurements showed extended dust shells around a sample of bright Mira variables and also allowed modeling of the dust characteristics. Radiative transfer models (Lopez et al. 1997) were used to retrieve physical parameters for the star itself (effective temperature and photospheric radius) and its surrounding dust envelope (inner/outer radius, inner radius temperature, and optical depth). Five of the observed stars (R Leonis, o Ceti, χ Cygni, U Orionis, and R Aquarii) are common to our sample. In all cases the dust shells detected by ISI around these stars are too cold at the condensation radius, and in any event too optically thin, to explain the variations we observe between K and L' (Mennesson 1999; P. Salomé et al. in preparation). So if dust layers are involved in the observed K' to L' discrepancy, they are different from the ones observed by the ISI, and there is no current evidence for their existence. Besides, we find large UD diameters increases between K' and L' even when no dust is detected close to the star by the ISI (Danchi et al. 1994), as in the case of χ Cygni and U Orionis. So we do not think that dust is likely to explain our results. Recent theoretical models do not predict a strong influence of dust on

interferometric measurements at near-infrared wavelengths (Bedding et al. 2001).

Physical stellar diameters derived by the ISI measurements at 11.15 μm before 1999 were still quite model-dependent, because the 13 m baseline visibilities were dominated by the dust-shell emission. More direct and accurate stellar diameter measurements were obtained in 1999 October/November on o Ceti close to maximum (average phase of 0.9) with a 56 m baseline. This baseline should completely resolve out the extended cool dust shell. Yet the derived UD stellar diameter of 48.2 ± 0.6 mas (Weiner et al. 2000) is much larger than what near-infrared measurements indicate: $\simeq$23–35 mas from J, H (Tuthill et al. 1999b), K' to L' (this work). This result is consistent with thermal emission from a hot extended (up to 2–3 stellar radii) region around the central photosphere that still contributes a significant part of the 11.15 μm mid-infrared coherent flux once the outer colder regions have been resolved out by the interferometer. It will be very interesting to compare our L' measurements to the ISI largest baseline observations of the same objects as they become available.

5. CONCLUSIONS

We have reported the first long-baseline interferometric measurements obtained in the 3.4–4.1 μm region on a sample of 14 asymptotic giant branch (AGB) stars, among which nine are Mira variables. They yield a systematic and rather surprising result: a strong increase in the apparent UD diameters of all the Mira variables from K' to L' bands. In the absence of obvious strong molecular absorption, the effective opacity in the broad-filter bandpasses may be determined by the continuum, or possibly by a pseudocontinuum, of weak lines. The observed diameter shift is therefore interpreted as a continuum effect. We suggest that a very extended ($\simeq$3 stellar photospheric radii) gas layer is responsible, as its contribution to the overall stellar flux increases with infrared wavelength.

We also suggest that this two-layer scenario explains the UD diameter chromatic variations already detected around a few of our sample objects by the Keck aperture-masking experiment from 1.5 to 3.08 μm and the yet larger diameter measured at 11.15 μm by heterodyne interferometry on o Ceti. Infrared spectra of many of our sample stars indicate that the outer layer is rich in molecular H_2O, so that H_2O could be an important source of opacity. But we still detect some chromatic size variations on one S-type star (χ Cygni). Interestingly, the K' to L' apparent UD diameter increase also occurs for four non-Mira stars, which suggests that large-amplitude pulsation is not required to produce the very extended, warm, and dense envelopes around Mira variables. Some other mechanism must be capable of producing this extension. If correct, the two-layer interpretation also means that Mira photospheres are significantly smaller than has been estimated from previous high angular resolution measurements. This could favor a fundamental mode of pulsation (Wood 1990).

Ground-based interferometric observations of late-type stars in the L' atmospheric window are of particular interest: they seem well suited to reveal and probe the extended layer in the upper atmosphere of these stars. At shorter wavelengths, the warm stellar photospheric emission and/or strong molecular absorption/diffusion dominate. At longer wavelengths, the cooler extended dust shell contaminates visibility measurements.

Finally, the warm extended layer discussed here could be of major interest for the understanding of mass-loss mechanisms at the end of the AGB phase. This intermediate extended region located between the hot photosphere and the cool outer dust shell provides ideal temperature and density conditions for complex chemistry to occur, including the slow nucleation of dust, driven farther away by stellar radiation pressure.

B. M. wishes to thank the Laboratoire d'Etudes Spatiales et d'Instrumentation en Astrophysique (former DESPA) at the Observatoire de Paris and the Institut National des Sciences de l'Univers for providing financial support to the TISIS experiment.

REFERENCES

Bedding, T., Jacob, A. P., Scholz, M., & Wood, P. R. 2001, MNRAS, 325, 1487
Beichman, C. A., Neugebauer, G., Habing, H. J., Clegg, T. E., & Chester, T. J. 1988, *IRAS* Catalogs & Atlases, Explanatory Supplement (Washington, DC: GPO)
Burns, D., et al. 1998, MNRAS, 297, 462
Chagnon, G., et al. 2001, AJ, in press
Coudé du Foresto, V., Perrin, G., Ruilier, C., Mennesson B., Traub, W., & Lacasse, M. 1998, Proc. SPIE, 3350, 854
Coudé du Foresto, V., Ridgway, S. T., & Mariotti, J. M. 1997, A&AS, 121, 379
Danchi, W. C., Bester, M., Degiacomi, C. G., Greenhill, L. J., & Townes, C. H. 1994, AJ, 107, 1469
Haniff, C. A., Scholz, M., & Tuthill, P. G. 1995, MNRAS, 276, 640
Hinkle, K. H., & Barnes, T. G. 1979, ApJ, 227, 923
Hofmann, K.-H., Scholz, M., & Wood, P. R. 1998, A&A, 339, 846
Le Bertre, T., & Winters, J. M. 1998, A&A, 334, 173
Little-Marenin, I. R., & Little, S. J. 1990, AJ, 99, 1173
Lopez, B., et al. 1997, ApJ, 488, 807
Loup, C., Forveille, T., Omont, A., & Paul, J. F. 1993, A&AS, 99, 291
Mennesson, B. 1999, Ph.D. thesis, Univ. Paris VII
Mennesson, B., et al. 1999a, A&A, 346, 181
———. 1999b, in ASP Conf. Ser. 194, Optical and IR Interferometry from Ground and Space, ed. S. C. Unwin & R. Stachnik (San Francisco: ASP), 194
Perrin, G. 1996, Ph.D. thesis, Univ. Paris VII
Perrin, G., Coudé du Foresto, V., Ridgway S., Mariotti, J. M., Traub, W. A., Carleton, N., & Lacasse, M. G. 1998, A&A, 331, 619
Perrin, G., et al. 1999, A&A, 345, 221
Quirrenbach, A., Mozurkewich, D., Armstrong, J. T., Buscher, D. F., & Hummel, C. A. 1993, ApJ, 406, 215
Schmidtke, P. C. 1987, in Cool Stars, Stellar Systems, and the Sun, ed. J. L. Linsky & R. E. Stencel (Berlin: Springer), 1
Scholz, M. 2001, MNRAS, 321, 347
Tej, A., Chandrasekhar, T., Ashok, N. M., Raglan, S., Richichi, A., & Stecklum, B. 1999, AJ, 117, 1857
Traub, W. A. 1998, in Proc. SPIE 3350, 848
Tsuji, T. 1988, A&A, 197, 185
Tsuji, T., Ohnaka, K., Aoki, W., & Yamamura, I. 1997, A&A, 320, 1
Tuthill, P. G., Danchi, W. C., Hale, D. S., Monnier, J. D., & Townes, C. H. 2000a, ApJ, 534, 907
Tuthill, P. G., Haniff, C. A., & Baldwin, J. E. 1995, MNRAS, 277, 1541
———. 1999a, MNRAS, 306, 353
Tuthill, P. G., Monnier, J. D., & Danchi, W. C. 1999b, in ASP Conf. Ser. 194, Optical and IR Interferometry from Ground and Space, ed. S. C. Unwin & R. Stachnik (San Francisco: ASP), 188
———. 2000b, Proc. SPIE, 4006, 491
Walker, H. J., & Cohen, M. 1988, AJ, 95, 1801
Weiner, J., Danchi, W. C., Hale, D. D. S., McMahon, J., Townes, C. H., Monnier, J. D., & Tuthill, P. G. 2000, ApJ, 544, 1097
Whitelock, P., & Feast, M. 2000, MNRAS, 319, 759
Willson, L. A. 2000, ARA&A, 38, 573
Wood, P. R. 1990, in From Miras to Planetary Nebulae, ed. M. O. Mennessier & A. Omont (Gif-sur-Yvette: Editions Frontières), 67
———. 1999, in IAU Symp. 191, Asymptotic Giant Branch Stars, ed. A. Lebre, T. Le Bertre, & C. Waelkens (San Francisco: ASP), 151
Yamamura, I., de Jong, T., & Cami, J. 1999, A&A, 348, L55
Young, J. S., et al. 2000, MNRAS, 318, 381